PAPER

Cost-effective estimation of single-mode thermal states by probabilistic quantum metrology

View the article online for updates and enhancements.

Quantum Science and Technology

Cost-effective estimation of single-mode thermal states by probabilistic quantum metrology

Massimo Frigerio[1,2,*] ⓘ, Stefano Olivares[1,2] ⓘ and Matteo G A Paris[1,2] ⓘ

[1] Quantum Technology Lab & Quantum Mechanics Group, Dipartimento di Fisica 'Aldo Pontremoli', Università degli Studi di Milano, I-20133 Milano, Italy
[2] Istituto Nazionale di Fisica Nucleare, Sezione di Milano, I-20133 Milano, Italy
* Author to whom any correspondence should be addressed.

E-mail: massimo.frigerio@unimi.it, stefano.olivares@fisica.unimi.it and matteo.paris@fisica.unimi.it

Abstract

In probabilistic quantum metrology, one aims at finding measurements that *concentrate* the Fisher information on the resulting conditional quantum states, i.e. those states post-selected according to the outcome of the measurement. The quantum Cramér–Rao (QCR) bound itself cannot be surpassed this way, but it could be possible to improve the information-cost ratio (where *cost* refers to the experimental implementation), or even the total Fisher information. In this paper, we propose a post-selection protocol achieving this goal using single-photon subtraction and thermal states of radiation. In particular, we achieve a larger information-cost ratio for the estimation of temperature than the strategy attaining the QCR bound. Our scheme involves only classical states of radiation and this contrasts with (but does not contradict) recent results proving that for *unitary* quantum statistical models, post-selection strategies can outperform direct protocols only exploiting nonclassical states.

1. Introduction and motivation

In the field of local quantum estimation theory, the quantum Cramér–Rao (QCR) bound, expressed in terms of the quantum Fisher information (QFI), gives the ultimate bound to the precision of any unbiased estimator of a single parameter describing a generic quantum statistical model [1–3]. The standard picture involves one-parameter continuous family of quantum states $\hat{\rho}_\lambda$ labeled by the values of λ. The quantum estimation problem aims at inferring the value λ by performing measurements on several copies of the state, and constructing an unbiased estimator out of the measurement outcomes. This process involves an optimization over all possible measurement strategies, i.e. all positive operator-valued measures (POVMs) on the Hilbert space of the system, whose solution is provided in terms of the symmetric logarithmic derivative (SLD).

A question arises on whether this bound can be exceeded by more elaborate measurement strategies that cannot be described by a (parameter-independent) POVM on the initial state, as for example measurements implemented by coupling the system with an ancilla and then measuring the ancilla in such a way that the conditional state of the system, post-selected according to the outcome of the measurement, gives an higher QFI for the parameter, as if the post-selection were able to concentrate the information in the final state: this is the framework of *probabilistic quantum metrology* [4–10]. However, general results show that these strategies cannot overcome the QCR bound [11–13], ultimately due to a compensation between the enhanced QFI of the post-selected states and the probability of success of the post-selection process. Moreover, the same conclusion holds true if one considers all the information available from the strategy, i.e. by adding to the count the Fisher information of the measurement's outcomes and the QFI of the discarded states of the system [14]. On the other hand, the optimal measurement specified by the SLD, despite fixing the ultimate quantum bound, is often unreasonable to implement in an experimental setting, which is the natural purpose of quantum metrology. Thus, at least two loopholes open in the above

argument. Firstly, probabilistic quantum metrology may actually achieve an advantage over the direct measurement procedure when sub-optimal, realistic measurement strategies are employed. This has been studied, e.g., in the context of the estimation of the gain of a nondeterministic linear amplifier [15], and in quantum magnetometry with nitrogen-vacancy centers of diamond [16]. Secondly, taking into account the experimental cost of implementing different detection methods, the overall information-cost ratio could be drastically improved by deciding to spend a higher amount of resources only in the trials with a successful post-selection outcome.

In this paper, we provide a detailed example to show that such advantages can indeed be achieved even when only classical states are involved, thereby excluding the necessity of any *quantumness* of the involved states to render post-selection profitable (*quantumness* of the measurement strategy may be still there). We consider a well known de-Gaussification protocol, i.e. single-photon subtraction, both with an ideal model and with a realistic implementation, applied to a thermal state of a single mode of radiation. We show that the ideal photon subtraction yields a non-Gaussian state with a higher QFI for the temperature parameter, suggesting a chance to overcome the QCR bound. However, single-photon subtraction is not a unitary operation. A standard experimental realization of the single-photon subtraction, which may be implemented with current quantum optical technology, involves sending the quantum state onto a beam splitter with very high transmissivity, and performing an on–off measurement on the weak, reflected beam: whenever the on–off detector clicks, it is very likely that a single photon has been detected and the transmitted state will approximate the photon-subtracted state. Thus, this is precisely an instance of probabilistic quantum metrology. Despite the no-go results discussed above, we show that already in this basic framework the two above alternatives allow us to obtain an advantage. In particular, if an heterodyne measurement protocol is assumed in place of the optimal photon-counting measurement needed to reach the QFI, the conditional strategy improves the total Fisher information for the temperature parameter. Moreover, taking into account the implementation cost of the different measurement schemes, the FI-to-resources ratio can dramatically improve using the realistic single-photon subtraction protocol.

The paper is structured as follows. In section 2 we establish notation and briefly summarize the properties of photon subtracted thermal states for both ideal and realistic single-photon subtraction. In section 3 we analyze in details the QFI of single-photon subtracted thermal states, whereas in section 4 we evaluate the FI of alternative, sub-optimal but realistic measurements, as homodyne, heterodyne, and on–off detection schemes. In section 5 we go back to the realistic single-photon subtraction scheme and illustrate how to extract the full information about the temperature, whereas in section 6 we perform a comparison among the different strategies in terms of the information-cost ratio. Section 7 closes the paper with some concluding remarks.

2. Photon subtracted thermal states

We begin by considering a thermal state of a single mode [17], characterized by an average number of photons $\lambda = (e^{\beta} - 1)^{-1}$, where $\beta = \hbar\omega/(k_B T)$, T is the temperature parameter of the state and ω is the frequency of the mode. In the number basis, the state can be expressed as:

$$\hat{\nu}_\lambda := \sum_{n=0}^{+\infty} p_n(\lambda)\, |n\rangle\langle n|, \tag{1}$$

$$p_n(\lambda) := \frac{1}{1+\lambda}\left(\frac{\lambda}{1+\lambda}\right)^n. \tag{2}$$

For the sake of analytic convenience, throughout the paper the parameter to be estimated will be λ rather than β^{-1}. Notice, however, that although the FIs for λ and β^{-1} are related by a temperature-dependent conversion factor dictated by propagation of uncertainty, this is the same factor for all the considered quantities, and it cannot influence the comparisons and the relevant conclusions we are going to draw. It is also worth mentioning that this state would describe the photon statistics of a single mode of radiation in thermal equilibrium *if it was emitted from a perfectly coherent source*.

2.1. Ideal single-photon subtraction

Ideally, the subtraction of a single photon is implemented on the Hilbert space by the action of the lowering operator $\hat{a}$ of the corresponding mode. If we denote $\hat{\nu}_\lambda^-$ the ideal single-photon subtracted thermal state, i.e.:

$$\hat{\nu}_\lambda^- := \mathcal{E}^-[\hat{\nu}_\lambda] = \frac{\hat{a}\,\hat{\nu}_\lambda\hat{a}^\dagger}{\text{Tr}[\hat{\nu}_\lambda\hat{a}^\dagger\hat{a}]} = \frac{1}{\lambda}\hat{a}\,\hat{\nu}_\lambda\hat{a}^\dagger. \tag{3}$$

its photon-number probability distribution will be:

$$p_n^-(\lambda) = \frac{n+1}{(1+\lambda)^2} \left(\frac{\lambda}{1+\lambda} \right)^n.$$
(4)

Notice that the average number of photons in the ideal single-photon subtracted thermal state is:

$$\mathrm{Tr}[\hat{\nu}_\lambda^- \hat{a}^\dagger \hat{a}] = 2\lambda$$

and, perhaps counter-intuitively, this is greater than λ, the average number of photons in the starting thermal state, before the ideal single-photon subtraction [18]. This is peculiar of the thermal distribution, and it can be partially understood by acknowledging that the vacuum state is always the most probable number state in a thermal distribution, and it is removed by the single-photon subtraction map. Notice also that the single-photon subtraction map does not preserve the energy.

We shall need to consider also other probability distributions associated with $\hat{\nu}_\lambda$ and $\hat{\nu}_\lambda^-$, whose expressions are easier to derive starting from an operator representation of these states. It is well known that a single mode thermal state can also be written as:

$$\hat{\nu}_\lambda = (1 - e^{-\beta})e^{-\beta \hat{a}^\dagger \hat{a}}.$$
(5)

Applying the ideal single-photon subtraction map $\mathcal{E}^-$ to this expression, we get:

$$\hat{\nu}_\lambda^- = (1 - e^{-\beta})^2 \left[\mathbb{I} + \hat{a}^\dagger \hat{a} \right] e^{-\beta \hat{a}^\dagger \hat{a}}$$

$$= (1 - e^{-\beta})^2 \left[\mathbb{I} - \frac{\partial}{\partial \beta} \right] e^{-\beta \hat{a}^\dagger \hat{a}}.$$
(6)

The last expression is very convenient to readily evaluate the homodyne and heterodyne distributions of $\hat{\nu}_\lambda^-$ from the well-known corresponding distributions of the thermal state $\hat{\nu}_\lambda$.

In a completely analogous way, the single-photon added thermal state defined by:

$$\hat{\nu}_\lambda^+ := \mathcal{E}^+ [\hat{\nu}_\lambda] = \frac{1}{\lambda + 1} \hat{a}^\dagger \hat{\nu}_\lambda \hat{a},$$
(7)

can be rewritten as:

$$\hat{\nu}_\lambda^+ = (e^\beta - 1)(1 - e^{-\beta}) \, \hat{a}^\dagger \hat{a} \, e^{-\beta \hat{a}^\dagger \hat{a}}$$

$$= -(e^\beta - 1)(1 - e^{-\beta}) \frac{\partial}{\partial \beta} e^{-\beta \hat{a}^\dagger \hat{a}}.$$
(8)

The corresponding photon-number distribution is:

$$p_n^+(\lambda) = \frac{n}{\lambda(1+\lambda)} \left(\frac{\lambda}{1+\lambda} \right)^n.$$
(9)

and the average photon number is $2\lambda + 1$ in this case.

The Husimi Q-function of these states are easily evaluated from equations (5), (6) and (7) with the help of the definition:

$$Q\left[\hat{\rho}\right](\alpha) := \frac{1}{\pi} \langle \alpha | \hat{\rho} | \alpha \rangle, \quad \alpha \in \mathbb{C}.$$
(10)

The results are as follows:

$$Q_\lambda(\alpha) = \frac{1}{\pi(1+\lambda)} \exp\left[-\frac{|\alpha|^2}{1+\lambda} \right],$$
(11)

$$Q_\lambda^-(\alpha) = \frac{1 + \lambda(1 + |\alpha|^2)}{\pi(1+\lambda)^3} \exp\left[-\frac{|\alpha|^2}{1+\lambda} \right],$$
(12)

$$Q_\lambda^+(\alpha) = \frac{|\alpha|^2}{\pi(1+\lambda)^2} \exp\left[-\frac{|\alpha|^2}{1+\lambda} \right].$$
(13)

In a completely analogous manner, it is possible to derive the probability distributions associated with the quadrature $\hat{x} = \frac{\hat{a} + \hat{a}^\dagger}{\sqrt{2}}$ on the states above. The results are:

$$X_\lambda(x) = \frac{1}{\sqrt{\pi}\sqrt{1+2\lambda}} \exp\left[-\frac{x^2}{1+2\lambda} \right],$$
(14)

$$X_\lambda^-(x) \;=\; \frac{1 + \lambda(3 + 2x^2 + 2\lambda)}{\sqrt{\pi}(1 + 2\lambda)^{5/2}} \, \exp\left[-\frac{x^2}{1 + 2\lambda}\right], \tag{15}$$

$$X_\lambda^+(x) \;=\; \frac{\lambda + 2(\lambda^2 + x^2(1 + \lambda))}{\sqrt{\pi}(1 + 2\lambda)^{5/2}} \, \exp\left[-\frac{x^2}{1 + 2\lambda}\right]. \tag{16}$$

It is worth mentioning that, among Gaussian measurements, either heterodyne detection (whose statistics is described by the Husimi Q-function) or homodyne detection are provably optimal to estimate the temperature of thermal states, as recently discussed in [19]. However, it is not obvious if this holds for the photon-subtracted and photon-added thermal states.

2.2. Realistic single-photon subtraction

Photon-subtraction is a cornerstone of many quantum optical protocols, and it is routinely exploited to prepare nonclassical and non-Gaussian states of light [20–24], as well as to test fundamental aspects of quantum mechanics [25–29] and to improve quantum teleportation with continuous variables [30, 31]. The standard way to implement approximate single-photon subtraction on a state in quantum optics involves sending it onto a high transmittance beam-splitter, with the vacuum state in the orthogonal port, and performing on–off detection on the weak, reflected signal [32]. In the limit of infinitesimal reflectivity of the beam-splitter and perfect efficiency of the on–off detection, whenever the detectors catches a signal, it will be a single photon and the transmitted, output state will be single-photon subtracted according to the ideal map $\mathcal{E}^-$ introduced above.

The action of the beam-splitter is described by the unitary operator:

$$\hat{U}_{\mathrm{BS}}(\zeta) := \exp\left[\zeta \hat{a}^\dagger \hat{b} - \zeta^* \hat{a} \hat{b}^\dagger\right]. \tag{17}$$

where $\hat{a}$ is the mode operator of the field we are interested in and $\hat{b}$ is the mode operator of the orthogonal port. The parameter $\zeta = \theta e^{i\phi}$ quantifies the transmissivity and the additional phase introduced by the beam-splitter. To explicitly carry out the calculations for generic values of beam-splitter transmissivity and detection efficiency, it is convenient to express the beam-splitter unitary evolution in the following form:

$$
\begin{aligned}
\hat{U}_{\mathrm{BS}}(\zeta) \;=\; & \exp\left[-e^{-i\phi} \tan\theta \; \hat{a}\hat{b}^\dagger\right] \left(\cos^2\theta\right)^{\frac{1}{2}(\hat{a}^\dagger\hat{a} - \hat{b}^\dagger\hat{b})} \\
& \times \exp\left[e^{i\phi} \tan\theta \; \hat{a}^\dagger\hat{b}\right].
\end{aligned}
\tag{18}
$$

which can be derived from the standard expression equation (17) by exploiting the rules of the two-boson representation of the $\mathfrak{su}(2)$ Lie algebra provided by the operators $\hat{J}_+ = \hat{a}^\dagger \hat{b}, \hat{J}_- = \hat{a}\hat{b}^\dagger$ and $\hat{J}_3 = \frac{1}{2}[\hat{J}_+, \hat{J}_-] = \frac{1}{2}(\hat{a}^\dagger\hat{a} - \hat{b}^\dagger\hat{b})$. For our realistic single-photon subtraction protocol we will assume $\phi = 0$ and $\eta = \cos^2\theta$ will be the beam-splitter *transmittance*. If $\theta = 0$, then $\eta = 1$ and $\hat{U}_{\mathrm{BS}} = \mathbb{I}$, so that the input state is fully transmitted.

As an input state, we shall take $\hat{\nu}_\lambda \otimes |0\rangle\langle 0|$, which is simply the thermal state to be analyzed on the first mode and the vacuum state in the other mode. It is now a simple matter to write down the output state of the two modes after the beam-splitter:

$$
\begin{aligned}
\hat{U}_{\mathrm{BS}}(\theta) \left[\hat{\nu}_\lambda \otimes |0\rangle\langle 0|\right] \hat{U}_{\mathrm{BS}}^\dagger(\theta) \;=\; & \frac{1}{1 + \lambda} \sum_{n=0}^{+\infty} \sum_{k,k'=0}^{n} \left(\frac{\lambda}{1 + \lambda}\right)^n \\
& \times \sqrt{\binom{n}{k}\binom{n}{k'}} (1 - \eta)^{\frac{k+k'}{2}} \eta^{n - \frac{k+k'}{2}} |n - k\rangle\langle n - k'| \otimes |k\rangle\langle k'|.
\end{aligned}
\tag{19}
$$

On this state, an on–off detection with efficiency $0 < \epsilon \leqslant 1$ is performed on the second mode. This is implemented at the mathematical level by a POVM with the following two operators:

$$\hat{\Pi}_0 = \sum_{m=0}^{+\infty} (1 - \epsilon)^m |m\rangle\langle m|, \tag{20}$$

$$\hat{\Pi}_1 = \mathbb{I} - \hat{\Pi}_0 \;=\; \sum_{m=0}^{+\infty} \left[1 - (1 - \epsilon)^m\right] |m\rangle\langle m|. \tag{21}$$

Whenever the detector clicks, meaning that the outcome is 1, the state of the first mode will be the approximate single-photon subtracted thermal state. This happens with probability:

$$
\begin{aligned}
\wp_1(\lambda; \eta, \epsilon) &= \mathrm{Tr}\left[\left(\mathbb{I} \otimes \hat{\Pi}_1\right) \hat{U}_{\mathrm{BS}}(\theta)\left[\hat{\boldsymbol{\nu}}_\lambda \otimes |0\rangle\langle 0|\right] \hat{U}_{\mathrm{BS}}^\dagger(\theta)\right] \\
&= \frac{\lambda\epsilon(1-\eta)}{1+\lambda\epsilon(1-\eta)}.
\end{aligned}
\tag{22}
$$

where we used a different calligraphic style for the letter 'p' to distinguish it from the photon-number distribution of the initial thermal state. If we denote by $\hat{\boldsymbol{\rho}}_\lambda$ the approximate single-photon subtracted thermal state and by Tr_B the partial trace over the second output mode of the beam-splitter, we can finally write:

$$
\begin{aligned}
\hat{\boldsymbol{\rho}}_\lambda &= \frac{1}{\wp_1} \mathrm{Tr}_B\left[\left(\mathbb{I} \otimes \hat{\Pi}_1\right) \hat{U}_{\mathrm{BS}}(\theta)\left[\hat{\boldsymbol{\nu}}_\lambda \otimes |0\rangle\langle 0|\right] \hat{U}_{\mathrm{BS}}^\dagger(\theta)\right] \\
&= \frac{1}{\wp_1} \frac{1}{1+\eta\lambda} \sum_{n=0}^{+\infty} \left(\frac{\eta\lambda}{1+\eta\lambda}\right)^n \\
&\quad \times \left[1 - \left(\frac{1+\eta\lambda}{1+\lambda(\eta+(1-\eta)\epsilon)}\right)^{n+1}\right] |n\rangle\langle n|.
\end{aligned}
\tag{23}
$$

The steps to arrive at this expression are easily reconstructed by rearranging the sums and applying the binomial theorem. Equation (23) has several interesting features: apart from the factor in square brackets and the normalization, the usual distribution of a thermal state with average number of photons $\eta\lambda$ can be clearly recognized: this would be the state of the first mode after the beam-splitter if no detection took place on the reflected beam. Moreover, both equation (19) and the final result in equation (23) involve P-classical states, in the sense of Glauber [33–36]. Indeed, the former is the result of a P-classical state mixed with the vacuum by a beam-splitter, while the final state is diagonal in the number basis and with non vanishing photon-number probability for any $n \geqslant 0$, hence it must be P-classical too; this also implies that their Wigner functions are everywhere non-negative in phase space. However, the state in equation (23) is non-Gaussian, having a Wigner function which is a linear combination of two Gaussians in phase space. This is due to the fact that, although the operator $\hat{\Pi}_0$ associated with the rejection of the selected state is Gaussian, the operator $\hat{\Pi}_1$ corresponding to the accepted state is not.

The fidelity between the realistic state equation (23) and the ideal one in equation (6) can be easily evaluated, albeit not in a closed form, exploiting the fact that they are both diagonal in the Fock basis and therefore it coincides with the classical fidelity of the photon-counting probability distributions. For the reference values used in our analysis, i.e. $\eta = 0.95$ and $\epsilon = 0.97$, the fidelity is greater than 0.9 for values of $\lambda \lesssim 70$.

3. Fisher information for single-photon subtracted thermal states

As a preliminary remark, we highlight the fact that all the states considered above are diagonal in the number basis, as in equations (1), (4), (9) and (23), whose vectors are independent of λ; therefore, the QFI of these states for the parameter λ reduces to the (classical) FI of their photon-number probability distributions, since the SLD is diagonal in the eigenbasis of the density matrix, whenever the eigenstates do not depend on the parameter. In other words, the problem of estimating λ on these states is a classical estimation problem embedded in a quantum setting. In this sense, single-photon detection is a *classical* detection strategy for this special scenario. Also, no entanglement is created by the beam-splitter, precisely because the input state is P-classical.

With the help of the standard formula for the FI for a parameter λ encoded in a probability distribution $P_k(\lambda)$ over a discrete random variable k:

$$
\begin{aligned}
\mathcal{F}[\{P_k(\lambda)\}] &:= \sum_k P_k(\lambda)\left[\partial_\lambda \log P_k(\lambda)\right]^2 \\
&= \sum_k \frac{[\partial_\lambda P_k(\lambda)]^2}{P_k(\lambda)}.
\end{aligned}
\tag{24}
$$

we arrive at the following expressions for the QFI $\mathcal{Q}$ of $\hat{\boldsymbol{\nu}}_\lambda, \hat{\boldsymbol{\nu}}_\lambda^-$ and $\hat{\boldsymbol{\nu}}_\lambda^+$, respectively,

$$
\mathcal{Q}[\hat{\boldsymbol{\nu}}_\lambda] = \mathcal{F}[p_n(\lambda)] = \frac{1}{\lambda(1+\lambda)},
\tag{25}
$$

$$
\mathcal{Q}[\hat{\boldsymbol{\nu}}_\lambda^-] = \mathcal{F}[p_n^-(\lambda)] = \frac{2}{\lambda(1+\lambda)} = \mathcal{Q}[\hat{\boldsymbol{\nu}}_\lambda^+].
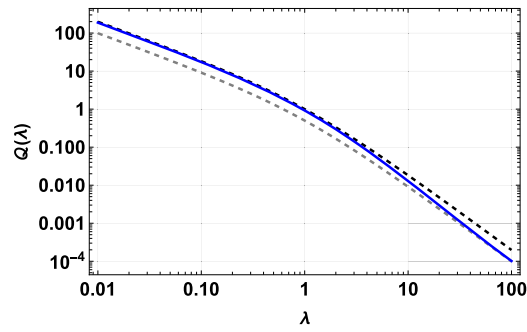\tag{26}
$$

Figure 1. QFI as a function of the average photon number $\lambda = (e^\beta - 1)^{-1}$ for thermal state (dashed gray), ideal single-photon subtracted/added thermal state (solid black) and realistic single-photon subtracted thermal state (blue) for a beam-splitter with transmittance $\eta = 0.95$ and on−off detection with efficiency $\epsilon = 0.99$. Mind the log-scale on both axes.

Thus we see that both ideal single-photon subtraction and addition double the QFI. The same computation for the more involved photon-number distribution of the realistic single-photon subtracted thermal state, equation (23) leads to a series that we were not able to sum in a closed form. However, by performing the sum numerically and plotting the resulting QFI as a function of λ against the results of equations (25) and (26), we confirmed that the advantage in the QFI can still be attained by the realistic single-photon subtraction protocol, as shown in figure 1 for plausible values of beam-splitter transmittance and detector efficiency ($\eta = 0.95$ and $\epsilon = 0.99$).

It can be seen that the QFI of the realistic single-photon subtraction converges to the ideal case in the limit $\lambda \to 0$: indeed, when the initial thermal state has a small average number of photons, the realistic protocol well-approximates the ideal scenario, because whenever the detector clicks, there is a high chance that just a single photon was actually caught. However, this is in spite of the probability of success $\wp_1(\lambda)$ of the protocol itself, and we shall consider this issue in a later section. When $\lambda \gg 1$, instead, the realistic single-photon subtracted thermal state performs no better than the initial thermal state itself.

4. Exploring other cost-effective measurement strategies

Despite the fact that the number basis is the one that translates our estimation task on thermal quantum states into a classical one, actually resolving the photon-number distribution is a formidable experimental work. Hence, it is interesting to study whether the advantage over the QFI of the unprocessed thermal state persists if we consider easier-to-implement measurements on the ideal and realistic single-photon subtracted thermal states.

We considered three detection strategies:

(a) **Homodyne detection** of the $\hat{x}$ quadrature, a standard detection protocol in quantum optics that involves combining the state with a reference coherent state (local oscillator) onto a 50/50 beam splitter and evaluating the difference between the photocurrents at the two outputs

(b) **Heterodyne detection** (or *double homodyne detection*) which effectively implements a POVM whose elements are coherent-state projectors

(c) **On−off detection** with efficiency ϵ, described by the POVM of equations (20) and (21) as before

Starting with homodyne measurements, figure 2 shows that it always performs worse than the QFI of the initial thermal state. However, the FI of the homodyne distributions X_λ^-, X_λ^+ and $\langle x|\hat{\rho}_\lambda|x\rangle$ are greater than the FI of X_λ over a wide range of values of λ, while for $\lambda \gg 50$ the approximate single-photon subtracted thermal state provides less information than the initial thermal state under homodyne detection.

Considering heterodyne detection instead, we found that $\hat{\nu}_\lambda^\pm$ and $\hat{\rho}_\lambda$ outperform even the QFI of the initial thermal state, in the range $\lambda \gtrsim 1$, while they perform better than the heterodyne distribution of $\hat{\nu}_\lambda$ for a greater range of values, but $\hat{\rho}_\lambda$ eventually becomes worse than $\hat{\nu}_\lambda$ for this detection strategy. These trends are displayed in figure 3.

Finally, let us discuss the cheapest strategy, on−off detection. With the idea of exploiting a resource we already harnessed, we will assume the detection efficiency to be the same of the on−off detection employed in the realistic single-photon subtraction protocol. In that case, the realistic scenario can be summarized by a black box with one input for the initial thermal state and two output for the signal of the two identical on−off detectors, put at the two ends of the beam-splitter. The signal of the first detector is recorded
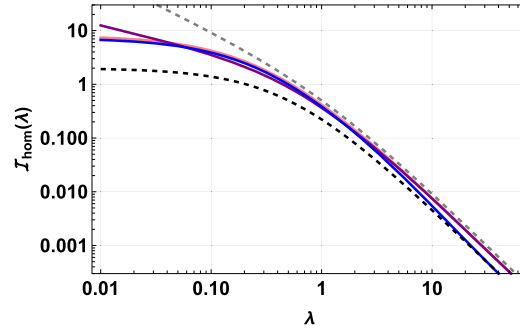
Figure 2. Fisher information of homodyne distribution as a function of the initial average photon number $\lambda = (e^\beta - 1)^{-1}$ for thermal states (dashed black), ideal single-photon subtracted/added thermal states (solid pink/purple) and realistic single-photon subtracted thermal states (solid blue) for a beam-splitter with transmittance $\eta = 0.95$ and on−off detection with efficiency $\epsilon = 0.97$. Mind the log-scale on both axes. QFI of thermal states (dashed gray) is also shown for reference.
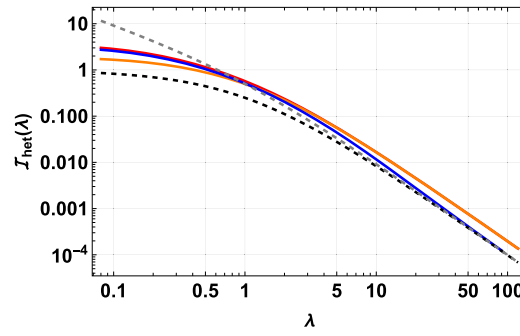

Figure 3. Fisher information of heterodyne distributions as a function of the initial average photon number $\lambda = (e^\beta - 1)^{-1}$ for thermal states (dashed black), ideal single-photon subtracted/added thermal states (solid red/orange) and realistic single-photon subtracted thermal states (solid blue) for a beam-splitter with transmittance $\eta = 0.95$ and on−off detection with efficiency $\epsilon = 0.97$. Mind the log-scale on both axes. QFI of thermal states (dashed gray) is also shown for reference.
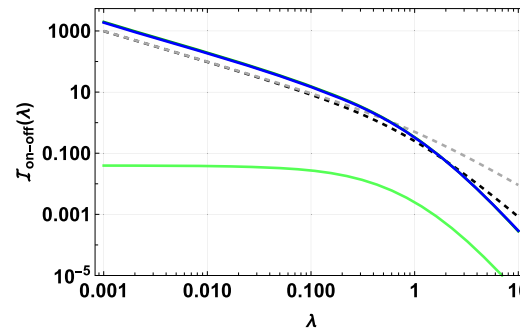

Figure 4. Fisher information of on−off distributions as a function of the initial average photon number $\lambda = (e^\beta - 1)^{-1}$ for thermal states (dashed black), ideal single-photon subtracted states (solid blue curve), photon-added thermal states (solid light-green) and realistic single-photon subtracted thermal states (solid blue curve, coinciding with the ideal photon-added state in this range) for a beam-splitter with transmittance $\eta = 0.95$ and on−off detection with efficiency $\epsilon = 0.97$. Mind the log-scale on both axes. QFI of thermal states (dashed gray) is also shown for reference.

whenever the second detector clicks, meaning that single-photon subtraction happened. This corresponds to relatively compact and easy-to-build apparatus.

Figure 4 shows that the FI of the on−off distributions for $\hat{\nu}_\lambda^-$ and $\hat{\rho}_\lambda$ are significantly greater than the QFI of the initial thermal state for $\lambda \lesssim 0.5$ and are still better than the FI of the on−off distribution of $\hat{\nu}_\lambda$ for $\lambda \lesssim 2$. On the other hand, the ideal photon-added state $\hat{\nu}_\lambda^+$ is completely inefficient with this detection strategy; the reason can be seen in the fact that the ideal photon-added state, unlike the initial thermal state, will almost always make an efficient on−off detector click, because it has no contribution from the vacuum state; therefore the on−off statistics will depend very weakly on the initial parameter of the thermal distribution.

5. Exploiting all the information from the realistic single-photon subtraction protocol

In evaluating the Fisher information of the probability distributions associated with the realistic single-photon subtracted thermal state, we disregarded a crucial issue: the realistic protocol is not always successful. If we repeat the protocol M times on identically prepared thermal states $\hat{\nu}_\lambda$, according to equation (22) we will prepare:

$$M' = M\wp_1(\lambda) = \frac{M\lambda\epsilon(1-\eta)}{1+\lambda\epsilon(1-\eta)}. \tag{27}$$

approximate single-photon subtracted thermal states $\hat{\rho}_\lambda$. Since the CR bound writes:

$$\text{Var}\left[\hat{\lambda}\right] \geqslant \frac{1}{M' \, \mathcal{F}[\hat{\rho}_\lambda]} = \frac{1}{M\wp_1(\lambda)\mathcal{F}[\hat{\rho}_\lambda]}. \tag{28}$$

for the variance of any unbiased estimator $\hat{\lambda}$ for the parameter λ, we deduce that having a reduced number of accepted single-photon subtracted thermal states effectively translates into a reduction of the Fisher information extractable by any measurement, by a λ-dependent factor which is precisely the probability of success $\wp_1(\lambda)$. However, stopping here would yield to a pessimistic underestimate: when the subtraction protocol fails, we still have a final state that can be measured. This is given by:

$$\hat{\rho}_\lambda^\varnothing = \frac{1}{\wp_0(\lambda)} \frac{1}{1+\lambda(\eta+(1-\eta)\epsilon)}$$
$$\times \sum_{n=0}^{+\infty} \left(\frac{\eta\lambda}{1+\eta\lambda+\lambda(1-\eta)\epsilon}\right)^n |n\rangle\langle n| \tag{29}$$

where $\wp_0(\lambda) = 1 - \wp_1(\lambda) = \frac{1}{1+\lambda(1-\eta)\epsilon}$. By writing:

$$\frac{\tilde{\lambda}}{\tilde{\lambda}+1} = \frac{\eta\lambda}{1+\eta\lambda+\lambda(1-\eta)\epsilon},$$

and solving for $\tilde{\lambda}$:

$$\tilde{\lambda} = \frac{\eta\lambda}{1+(1-\eta)\epsilon\lambda}, \tag{30}$$

we can rewrite equation (29) as:

$$\hat{\rho}_\lambda^\varnothing = \frac{1}{1+\tilde{\lambda}}\sum_{n=0}^{+\infty} \left(\frac{\tilde{\lambda}}{1+\tilde{\lambda}}\right)^n |n\rangle\langle n|. \tag{31}$$

Thus, whenever the realistic single-photon subtraction protocol fails, the resulting state is again a thermal state, but with a new average photon number $\tilde{\lambda}$. The QFI with respect to λ of $\hat{\nu}_{\tilde{\lambda}}$ will therefore be:

$$\mathcal{Q}\left[\hat{\nu}_{\tilde{\lambda}};\lambda\right] = \left(\frac{\partial\tilde{\lambda}}{\partial\lambda}\right)^2 \mathcal{Q}\left[\hat{\nu}_{\tilde{\lambda}};\tilde{\lambda}\right]$$
$$= \frac{\eta}{(1+\epsilon(1-\eta)\lambda)^2}\frac{1}{\lambda(1+\eta\lambda+(1-\eta)\epsilon\lambda)} \tag{32}$$

which is smaller than $\mathcal{Q}\left[\hat{\nu}_\lambda;\lambda\right]$, the QFI of the starting thermal state. Finally, additional information is provided by the very same probability distribution of success for the approximate single-photon subtraction. Specifically, the corresponding FI is:

$$\mathcal{F}\left[\{\wp_0,\wp_1\}\right] = \frac{(\partial_\lambda\wp_1)^2}{\wp_1} + \frac{(\partial_\lambda\wp_0)^2}{\wp_0}$$
$$= \frac{\epsilon(1-\eta)}{\lambda(1+\lambda\epsilon(1-\eta))^2}. \tag{33}$$

Overall, the full information that we can extract from the approximate single-photon subtraction protocol on $\hat{\nu}_\lambda$, assuming the best possible detection strategy on the output states, is [12]:

$$\mathcal{F}_{\text{tot}} := \mathcal{F}[\{\wp_0,\wp_1\}] + \wp_1\mathcal{Q}[\hat{\rho}_\lambda] + \wp_0\mathcal{Q}\left[\hat{\rho}_\lambda^\varnothing\right]. \tag{34}$$
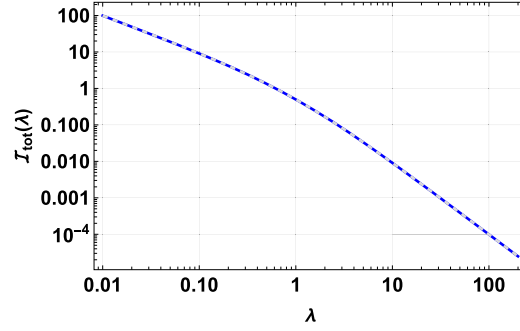
Figure 5. Total information $\mathcal{F}_{tot}$ on λ extractable from the realistic single-photon subtraction protocol on $\hat{\nu}_\lambda$ (solid blue) for a beam-splitter with transmittance $\eta = 0.95$ and on−off detection with efficiency $\epsilon = 0.97$, vs QFI of the original thermal state $\hat{\nu}_\lambda$ (dashed gray).

This is plotted against the reference quantity $\mathcal{Q}[\hat{\nu}_\lambda]$ in figure 5.

It appears as if all the advantage we found with the realistic single-photon subtracted thermal state is precisely canceled by the weighted sum in equation (34), so that the total extractable information comes to coincide with the initial QFI of $\hat{\nu}_\lambda$ (a similar result for photon-subtraction on Gaussian states was found in [37]). This can be understood by noting that $\mathcal{F}_{tot}$ is necessarily upper-bounded by the QFI of the output state of the beam splitter before the post-selection, equation (19), since all the collected outcomes (including the one encoded in the acceptance probability) can be viewed as a single string of outcome for a measurement performed on the joined state of the two output modes. But this is simply the result of the BS unitary evolution of the vacuum with the initial state whose temperature we wanted to estimate, therefore the QFI for the temperature parameter will be the same as for the thermal state we started with.

One can also derive a lower bound on $\mathcal{F}_{tot}$, taking advantage of a convexity property of the QFI [38]: if a family ϱ_λ of quantum states encoding a parameter λ is decomposed into a convex mixture according to:

$$\varrho_\lambda = \sum_a p_\lambda^a \varrho_\lambda^a \tag{35}$$

where p_λ^a is a probability distribution over the variable a, depending upon the parameter λ, then:

$$\mathcal{Q}[\varrho_\lambda] \leqslant \sum_a p_\lambda^a \mathcal{Q}[\varrho_\lambda^a] + \mathcal{F}[\{p_\lambda^a\}]. \tag{36}$$

This is called an *extended convexity property* for the QFI, since it states that the QFI of a mixture is no greater than the average of the QFI of the states in the ensemble *plus* the classical FI of the probability distribution of the ensemble. For us, the convex combination is:

$$\varrho_\lambda = \wp_1(\lambda)\hat{\rho}_\lambda + \wp_0(\lambda)\hat{\rho}_\lambda^\varnothing = \hat{\nu}_{\eta\lambda} \tag{37}$$

which is simply the statement that if we ignore the outcome of the on−off detector in the realistic single-photon subtraction protocol, the outcome will be again a thermal state, with an average number of photons reduced by the beam-splitter transmittance: $\eta\lambda$. The extended convexity property (36) then implies:

$$\mathcal{Q}[\hat{\nu}_{\eta\lambda}; \lambda] = \frac{\eta}{\lambda(1 + \eta\lambda)} \leqslant \mathcal{F}_{tot}. \tag{38}$$

As $\eta \to 1$, the lower bound converges to the QFI of $\hat{\nu}_\lambda$, while in general, for $0 < \eta < 1$, we have:

$$\frac{\eta}{\lambda(1 + \eta\lambda)} < \frac{1}{\lambda(1 + \lambda)} = \mathcal{Q}[\hat{\nu}_\lambda]. \tag{39}$$

The fact that the metrological advantage of realistic single-photon subtracted thermal state cannot be actually harnessed with the optimal detection strategy, i.e. photon-number detection, is of minor hindrance from a practical perspective, since photon-number detection is experimentally very challenging anyway. Therefore it is meaningful to explore whether the total extractable information from the realistic single-photon subtracted thermal state can be larger than the FI of the initial state for sub-optimal, but experimentally more relevant detection strategies.

In figure 6 we plotted the total information retrieved by the realistic photon-subtraction scheme, but assuming *heterodyne detection* on the output states of the beam splitter (blue curve), compared to the Fisher information for the heterodyne distribution of the initial thermal state. For $\lambda \lesssim 0.3$, the post-selection
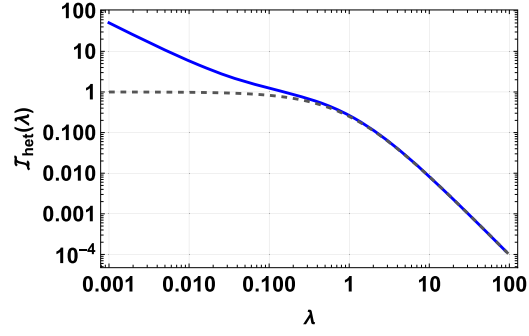
Figure 6. Total information retrieved from realistic photon-subtraction protocol followed by heterodyne detection of the output (blue curve) and Fisher information of the heterodyne distribution of $\hat{\nu}_\lambda$ for comparison (dashed, gray curve). The detection efficiency of the on−off measurement is $\epsilon = 0.99$ and the transmittance of the BS is $\eta = 0.95$.

Figure 7. Total information retrieved from realistic photon-subtraction protocol followed by on−off detection of the output (blue curve) and Fisher information of the heterodyne distribution of $\hat{\nu}_\lambda$ for comparison (dashed, gray curve). The detection efficiency of the on−off measurements is $\epsilon = 0.99$ and the transmittance of the BS is $\eta = 0.95$.
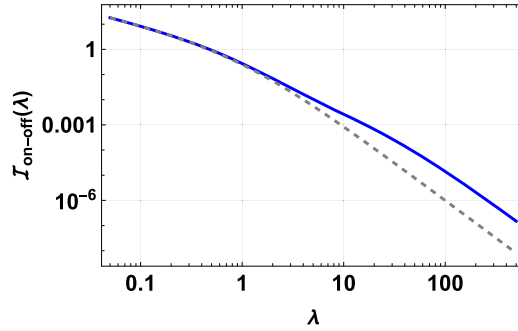
provides larger information, even taking into account the photon-subtraction probabilities. Analogously, in figure 7, both for the post-selection scenario (blue curve) and for the one without post-selection (gray, dashed curve), we chose as final measurement an on−off photon detection with the same efficiency $\epsilon = 0.99$. Now the advantage of the conditional strategy is seen for $\lambda \gtrsim 2$.

6. Information-cost ratio

In order to take into account the amount of resources required to implement the different detection schemes, let us introduce the so-called *cost parameters* [8, 39]. We denote by C_P the cost of the preparation of the initial quantum state, by C_S the cost of the post-selection process (i.e., essentially that of an on−off measurement) and by C_M the cost of the final measurement which, when photon-subtraction is considered, is performed only when the post-selection is effective. Whenever the post-selection fails, we will perform the least expensive measurement, which is on−off detection with the same efficiency ϵ, on the resulting state $\hat{\rho}_\lambda^\varnothing$. The Fisher information, with respect to the initial parameter λ, extractable from the resulting statistics is readily calculated:

$$\mathcal{F}^\varnothing = \frac{\epsilon \eta}{\lambda (1 + \epsilon \lambda)^2 (1 + \epsilon (1 - \eta) \lambda)}. \tag{40}$$

The information-cost ratio for the post-selection strategy, $\mathcal{R}_{ps}$, is then given by [8, 39]:

$$\mathcal{R}_{ps} = \frac{\wp_1 \mathcal{F}_M [\hat{\rho}_\lambda] + \wp_0 \mathcal{F}^\varnothing + \mathcal{F} [\{\wp_0, \wp_1\}]}{C_P + C_S + \wp_1 C_M + \wp_0 C_S}. \tag{41}$$

where $\mathcal{F}_M [\hat{\rho}_\lambda]$ is the Fisher information for the measurement strategy labeled by M performed on the successfully post-selected state $\hat{\rho}_\lambda$ and we attributed the same post-selection cost C_S also to the on−off measurement on the rejected state with the $\wp_0 C_S$ term in the denominator. In the standard quantum estimation protocol, without performing the photon-subtraction, the information-cost ratio would be:

$$\mathcal{R}_0 = \frac{\mathcal{F}_M [\hat{\nu}_\lambda]}{C_P + C_M}. \tag{42}$$
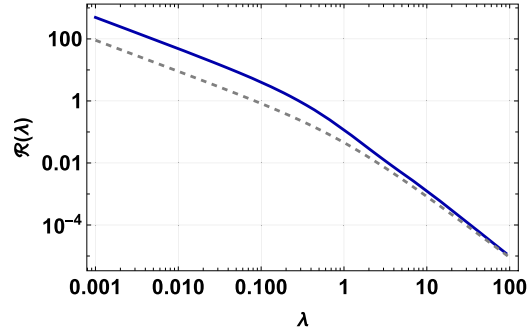
Figure 8. Information-cost ratio for the realistic photon subtraction protocol followed by homodyne detection ($\mathcal{R}_{ps}$, solid blue curve) and for the initial thermal state subjected to the optimal photon-number measurement ($\mathcal{R}_0$, dashed gray curve), as functions of the parameter λ to be estimated. The cost of preparation was assumed to be $C_P = 1$, that of post-selection $C_S = 0.5$ and the measurement cost is $C_M = 10$. The detection efficiency of the on−off measurements is $\epsilon = 0.99$ and the transmittance of the BS is $\eta = 0.95$.
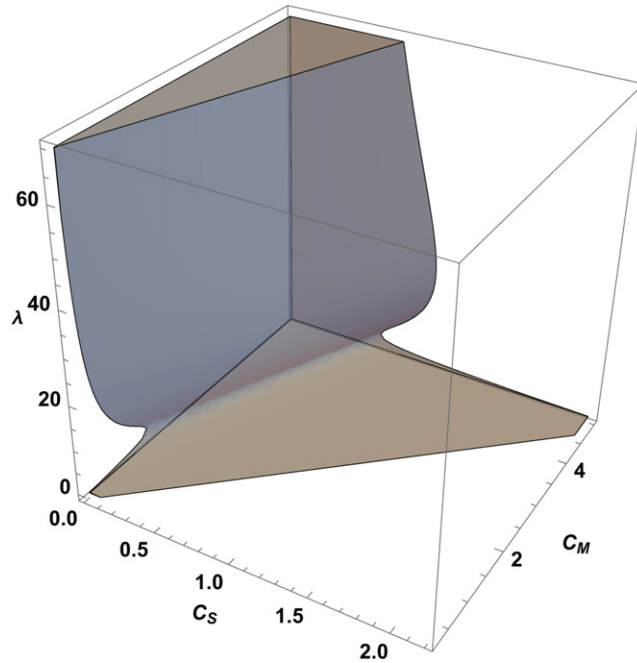

Figure 9. Region in parameters space of C_S, C_M and λ where $\mathcal{R}_{ps} > \mathcal{R}_0$, implying that the probabilistic protocol is better from a cost-effective standpoint. We fixed $C_P = 1$ without loss of generality, since only the ratios between the other costs and C_P can influence the inequality.

Since C_M is usually the largest among the costs and the realistic photon-subtraction strategy pays it only for the more informative states $\hat{\rho}_\lambda$, it is clear that it is possible to have $\mathcal{R}_{ps} > \mathcal{R}_0$. To provide just an example of this fact, let us assume $C_P = 1$, $C_S = 0.5$ and $C_M = 10$. We will take the same C_M both for $\mathcal{R}_{ps}$ and $\mathcal{R}_0$, but we will assume heterodyne detection on $\hat{\rho}_\lambda$ and the optimal, photon-number measurement on $\hat{\nu}_\lambda$ (so that $\mathcal{F}_M[\hat{\nu}_\lambda] = \mathcal{Q}[\hat{\nu}_\lambda]$). This is perhaps unrealistic, since a measurement that has to resolve the full photon-number distribution will be more difficult to perform than heterodyne detection, however it makes our point even stronger, since if $\mathcal{R}_{ps} > \mathcal{R}_0$ when the measurement costs are considered the same, it will be true *a fortiori* when more plausible values are inserted. The comparison is depicted (in logarithmic scale) in figure 8 as a function of λ, where the blue curve refers to $\mathcal{R}_0$ and the dashed gray curve to $\mathcal{R}_{ps}$.

Clearly, at least for low temperature thermal states, the realistic photon-subtraction strategy followed by heterodyne detection has a better information-cost ratio than the optimal measurement on the initial thermal state that achieves the QCR bound. The term $\wp_0 \mathcal{F}^\oslash$ in the numerator of $\mathcal{R}_{ps}$ is typically negligible, and one can work with the more compact expression

$$\mathcal{R}_{ps} \simeq (\wp_1 \mathcal{F}_M[\hat{\rho}_\lambda] + \mathcal{F}[\{\wp_0, \wp_1\}])/(C_P + C_S + \wp_1 C_M).$$

On the other hand, it would be meaningless to discard the $\mathcal{F}\left[\{\wp_0, \wp_1\}\right]$ term, since this information is already available anyway. In figure 9, we plotted the region in the parameters space of C_S, C_M and λ where $\mathcal{R}_{ps} > \mathcal{R}_0$ to show that the choice of the costs is not too critical for our result, for most values of λ.

Finally, let us remark that, for $\lambda \ll 1$, there is always a cheap, very effective strategy, which is to perform an on–off measurement directly on $\hat{\nu}_\lambda$; indeed, such a measurement yields a good approximation to the full photon-number distribution in that limit. However, this strategy is doomed to failure for large enough values of λ, implying that our post-selection protocol is the most efficient of all the considered ones in a wide range of temperatures.

7. Conclusions and remarks

In this paper, we have explored the effectiveness of single-photon subtraction in enhancing the QFI for the temperature parameter [40] of a thermal state of a single mode of radiation. After arguing that ideal single-photon subtraction is indeed effective, we have considered a practical implementation involving a highly transmitting beam splitter and an on–off detection on the reflected beam. This setup naturally shifts the focus to the field of probabilistic quantum metrology, which deals with measurements and post-selection strategies to concentrate the information on the output quantum state before the final measurement. Although no overall enhancement of the QFI persists once all the contributions to the extractable information from the probabilistic protocol are taken into account, this conclusion holds true only if the ability to perform the optimal measurement, required to achieve the QFI, is assumed. Since this request is often too demanding, we have examined other measurement protocols on the final states, such as heterodyne and homodyne detection. An actual advantage of these strategies over the straightforward optimal measurement on the initial thermal state is certified by looking at the information-cost ratio, which is given by the total Fisher information divided by the sum of the costs of all the involved resources (preparation of the initial state, final measurement and, possibly, post-selection). In particular, we have shown that, under very conservative values of the costs, realistic single-photon subtraction (followed by heterodyne measurement on the output when the subtraction is successful), yields an higher information-cost ratio than the standard optimal strategy required to achieve the QCR bound.

We remark that we adopted the framework of *local* quantum metrology, but our results indicate that the optimal measurement can be determined with very limited *a priori* knowledge of the true value of the parameter λ. Recently, a paradigm for global quantum thermometry has also been considered in this regard [41].

It should be noticed that viable techniques to achieve *deterministic* single-photon subtraction have been devised (see e.g. [42–44] and references therein) and, in light of our results, it is conceivable that they would permit to go beyond the QCR bound in the temperature estimation of a thermal state of radiation. On the other hand, these procedures are significantly more contrived than the cheap beam-splitter protocol that we have assumed, and the costs should be reconsidered accordingly.

We also notice that in our analysis the average number of photon is the parameter we are going to estimate and not a measure of the involved resources. The plots where the Fisher (and quantum Fisher) information is reported as a function of λ should not be intended to assess the performance at fixed resources. Rather, they reflect that the problem is not covariant [2], and therefore precision depends on the value of the parameter itself. Here, the comparison among the different strategies, which themselves involve a different amount of operational resources, has been done using the concept of cost parameter.

Finally, our analysis complements and contrasts with a recent work [39] in which the authors prove the necessity of a form of nonclassicality, namely the negativity of a generalized Kirkwood–Dirac distribution, to achieve an improvement of the information-cost ratio with post-selection (see also [45]). In our case, no form of state nonclassicality is at play, because we are always dealing with fully classical states according to Glauber's definition, which is widely regarded as the most general notion of nonclassicality (but we also refer to [46] for subtle issues in this respect, especially when weak measurements are involved). This does not contradict the results of [39], since they considered *unitary* quantum estimation problems and the consequent maximization over the probing state at the input of the unitary channel, while temperature cannot be considered a unitarily-imprinted parameter and no further maximization can be made. Therefore, the present work shows that the restriction in [39] to unitarily-imprinted parameters is actually necessary to arrive at their conclusion and, with more general assumptions, an improvement of the information-cost ratio with probabilistic metrology is possible also with classical probes. In this respect, we remind that our goal has not been to determine the absolute best strategy to estimate the temperature of a thermal light state, but rather to lay down a full example that shows the actual advantages that probabilistic (quantum) metrology can provide even without the need of nonclassical states.

Acknowledgments

Data availability statement

The data that support the findings of this study are available upon reasonable request from the authors.

ORCID iDs

Massimo Frigerio ⬤ https://orcid.org/0000-0002-2821-0574
Stefano Olivares ⬤ https://orcid.org/0000-0002-9251-0731
Matteo G A Paris ⬤ https://orcid.org/0000-0001-7523-7289

References

[1] Helstrom C W 1976 *Quantum Detection and Estimation Theory* (New York: Academic)
[2] Paris M G A 2009 *Int. J. Quantum Inf.* **07** 125
[3] Giovannetti V, Lloyd S and Maccone L 2011 *Nat. Photon.* **5** 222
[4] Fiurášek J 2006 *New J. Phys.* **8** 192
[5] Gendra B, Ronco-Bonvehi E, Calsamiglia J, Muñoz-Tapia R and Bagan E 2013 *Phys. Rev. Lett.* **110** 100501
[6] Calsamiglia J, Gendra B, Muñoz-Tapia R and Bagan E 2016 *New J. Phys.* **18** 103049
[7] Magaña-Loaiza O S, Harris J, Lundeen J S and Boyd R W 2016 *Phys. Scr.* **92** 023001
[8] Combes J and Ferrie C 2015 *Phys. Rev. A* **92** 022117
[9] Li G, Chen L-B, Wang T, He Z-H and Song H-S 2019 *J. Phys. B: At. Mol. Opt. Phys.* **52** 155501
[10] Chen G, Yin P, Zhang W-H, Li G-C, Li C-F and Guo G-C 2021 *Entropy* **23** 354
[11] Tanaka S and Yamamoto N 2013 *Phys. Rev. A* **88** 042116
[12] Zhang L, Datta A and Walmsley I A 2015 *Phys. Rev. Lett.* **114** 210801
[13] Ferrie C and Combes J 2014 *Phys. Rev. Lett.* **112** 040406
[14] Combes J, Ferrie C, Jiang Z and Caves C M 2014 *Phys. Rev. A* **89** 052117
[15] Adnane H, Albarelli F, Gharbi A and Paris M G A 2019 *J. Phys. A: Math. Theor.* **52** 495302
[16] Coto R, Dinani H T, Norambuena A, Chen M and Maze J R 2021 *Quantum Sci. Technol.* **6** 035011
[17] Olivares S 2021 *Phys. Lett. A* **418** 127720
[18] Mizrahi S S and Dodonov V V 2002 *J. Phys. A: Math. Gen.* **35** 8847
[19] Cenni M F B, Lami L, Acin A and Mehboudi M 2021 Thermometry of Gaussian quantum systems using Gaussian measurements (arXiv:2110.02098 [quant-ph])
[20] Ourjoumtsev A, Tualle-Brouri R, Laurat J and Grangier P 2006 *Science* **312** 83
[21] Ourjoumtsev A, Dantan A, Tualle-Brouri R and Grangier P 2007 *Phys. Rev. Lett.* **98** 030502
[22] Wenger J, Tualle-Brouri R and Grangier P 2004 *Phys. Rev. Lett.* **92** 153601
[23] Fiurášek J, García-Patrón R and Cerf N J 2005 *Phys. Rev. A* **72** 033822
[24] Olivares S and Paris M G A 2005 *J. Opt. B: Quantum Semiclass. Opt.* **7** S616
[25] Parigi V, Zavatta A, Kim M and Bellini M 2007 *Science* **317** 1890
[26] Zavatta A, Parigi V, Kim M S and Bellini M 2008 *New J. Phys.* **10** 123006
[27] Olivares S and Paris M G A 2004 *Phys. Rev. A* **70** 032112
[28] Olivares S and Paris M G A 2005 *J. Opt. B: Quantum Semiclass. Opt.* **7** S392
[29] Invernizzi C, Olivares S, Paris M G A and Banaszek K 2005 *Phys. Rev. A* **72** 042105
[30] Opatrný T, Kurizki G and Welsch D-G 2000 *Phys. Rev. A* **61** 032302
[31] Olivares S, Paris M G A and Bonifacio R 2003 *Phys. Rev. A* **67** 032314
[32] Barnett S M, Ferenczi G, Gilson C R and Speirits F C 2018 *Phys. Rev. A* **98** 013809
[33] Glauber R J 1963 *Phys. Rev.* **131** 2766
[34] Sudarshan E C G 1963 *Phys. Rev. Lett.* **10** 277
[35] Cahill K E and Glauber R J 1969 *Phys. Rev.* **177** 1857
[36] Glauber R J 1969 *Phys. Rev. A* **131** 1882
[37] Braun D, Jian P, Pinel O and Treps N 2014 *Phys. Rev. A* **90** 013821
[38] Alipour S and Rezakhani A T 2015 *Phys. Rev. A* **91** 042104
[39] Arvidsson-Shukur D R M, Halpern N Y, Lepage H V, Lasek A A, Barnes C H W and Lloyd S 2020 *Nat. Commun.* **11** 3775
[40] To be precise, we have referred to the parameter to be estimated as the *temperature* even if we have always used the average photon number $\lambda = (e^{\beta} - 1)^{-1}$, while the actual temperature of the thermal state is (proportional to) β^{-1}. This is not affecting our conclusions, see section 2.
[41] Rubio J, Anders J and Correa L A 2021 *Phys. Rev. Lett.* **127** 190402
[42] Rosenblum S, Bechler O, Shomroni I, Lovsky Y, Guendelman G and Dayan B 2015 *Nat. Photon.* **10** 19
[43] Honer J, Löw R, Weimer H, Pfau T and Büchler H P 2011 *Phys. Rev. Lett.* **107** 093601
[44] Du J, Li W and Bajcsy M 2020 *Opt. Express* **28** 6835
[45] Das S, Modak S and Bera M N 2021 Bounding quantum advantages in postselected metrology (arXiv:2108.09220 [quant-ph])
[46] Johansen L M 2004 *J. Opt. B: Quantum Semiclass. Opt.* **6** L21